PHYSICAL REVIEW A VOLUME 57, NUMBER 3 MARCH 1998

Double photoionization of helium from threshold to high energies

Yanghui Qiu, Jian-Zhi Tang, and Joachim Burgdörfer
Department of Physics, University of Tennessee, Knoxville, Tennessee 37996-1200
and Oak Ridge National Laboratory, Oak Ridge, Tennessee 37831-6377

Jianyi Wang
Department of Physics, Tulane University, New Orleans, Louisiana 70118
(Received 30 May 1997)

We present accurate calculations for the single and double photoionization of helium from the threshold to the high-energy limit. At low and intermediate energies, we use the *ab initio* hyperspherical close-coupling method, which is extended up to 1 keV by introducing an energy-dependent reaction region. At high energies we employ an *accurate* Hylleraas initial state and a 3*C* correlated final-state wave function. The 3*C* wave function is shown to be correct to leading order in Z/k. We find good agreement with recent experiments over the entire energy range. The two calculations merge at $\sim$1 keV to within 5%. [S1050-2947(98)50603-8]

PACS number(s): 32.80.Fb, 31.15.Ja, 31.25.−v

The double ionization of helium by photoabsorption provides a sensitive test for electron-electron correlations. Because the coupling between the electron and the radiation field ($\propto \mathbf{p}\cdot\mathbf{A}$) is a one-body operator, the simultaneous ejection of two electrons by one photon is mediated through the electron-electron interaction in the initial state (''ground-state correlation'') and/or in the final state of two electrons in the Coulomb continuum (''final-state correlation''). A large number of recent experimental (see, e.g., Refs. [1–4]) and theoretical [5–11] studies have investigated the ratio $R_{\rm ph}=\sigma^{++}/\sigma^{+}$ of double to single ionization for photon energies from near threshold (photon energy $E_{\rm ph}\approx 80$ eV) to high energies ($\sim$keV). For low photon energies $E_{\rm ph}\leqslant 300$ eV accurate *ab initio* methods, such as the hyperspherical close-coupling (HSCC) [9], R-matrix [10], and complex Sturmian [11] methods have been recently developed, which have led to improved agreement with most recent measurements. In the high-energy region several approaches have been pursued, including many-body perturbation theory (MBPT) [12,13], the use of the correlated 3C wave function as the final state [6,8,14] and, very recently, the use of the dipole response function [15]. In this regime, discrepancies between different theoretical predictions have remained unresolved and the comparison with experiments is complicated by the fact that in some experiments the separation of Compton scattering from photoionization was not performed. Moreover, at intermediate energies ($\geqslant$400 eV) no reliable calculations are available.

In this Rapid Communication we present a *comprehensive* calculation from the *threshold to high energies* by employing two complementary methods. From low to intermediate energies, we use the accurate HSCC method [9] and extend it to energies up to 1 keV by using a large number of channels ($\approx$175) and an energy-dependent matching hyperradius describing the reaction zone. At high energies, we show that the 3*C* wave function [17] (i.e., a product of three Coulomb functions) is the solution of the three-body Schrödinger equation to order Z/k_1 (Z, nuclear charge; k_1, momentum of the outgoing fast electron) in the relevant region of coordinate space, where the dominant contributions to the dipole matrix element originate, and discuss the likely source of discrepancies in previous calculations. At about 1 keV the two approaches merge with a relative deviation of about 5%.

A detailed description of the HSCC method is given in Refs. [9,16]. Briefly, the HSCC method for two-electron systems proceeds by dividing the six-dimensional (6D) configuration space into an inner region with hyperradius $R=(r_1^2+r_2^2)^{1/2}\leqslant R_M$ and an outer region where the asymptotic wave functions are expressed as

$$\Phi_j^{(\rm out)}=r_>^{-1}\sum_i \phi_i(\mathbf{r}_<,\hat{r}_>)[f_i(r_>)\delta_{ij}-g_i(r_>)K_{ij}], \quad (1)$$

where K is the reactance matrix, $f(g)$ is the regular (irregular) Coulomb function, and ϕ_i is defined as

$$\phi_i=R_{\tilde{n}l}(r_<)Y_{LM}(\hat{r}_1,\hat{r}_2). \quad (2)$$

Here, the Y_{LM} is the coupled two-electron spherical harmonics and $R_{\tilde{n}l}(r_<)$ is a radial function of the hydrogenic He^+ ion confined to a box of size $r_M=R_M/\sqrt{2}$, i.e.,

$$R_{\tilde{n}l}(r_M)=0. \quad (3)$$

Eigenfunctions $R_{\tilde{n}l}$ with eigenenergies $\epsilon_{\tilde{n}l}<0$ represent bound states and, hence, excitation-ionization channels, while eigenfunctions with $\epsilon_{\tilde{n}l}>0$ represent the discretized double-ionization continuum (see Fig. 1). In the inner region, the Schrödinger equation is solved by a close-coupling expansion in hyperspherical coordinates

$$\Phi_{(E)}^{(\rm in)}(R,\alpha,\Omega)=\sum_\mu F_\mu^{(E)}(R)\phi_\mu(R;\alpha,\Omega), \quad (4)$$

where $\alpha=\arctan(r_2/r_1)$ is the hyperangle, Ω denotes collectively the four angles $(\hat{r}_1,\hat{r}_2)$, and ϕ_μ represents the *diabatic* channel functions. The latter are solutions of the diagonal part of the Hamiltonian at a fixed hyperradius R for each

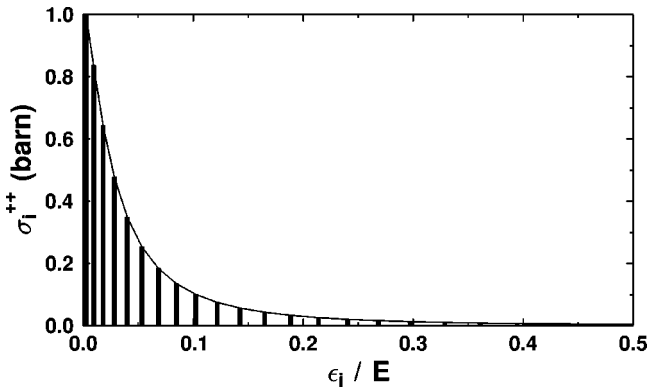

FIG. 1. Energy sharing of the two electrons at photon energy $E_{\rm ph}=1$ keV. The ϵ_i represents the eigenenergies of the discretized pseudostates confined within a box of $R_M=20$.

angular-momentum pair (l_1,l_2). The nondiagonal interaction contributes to the coupling matrix $V_{\mu\nu}$ of the close-coupling equation [16],

$$\left(-\frac{1}{2}\frac{\partial^2}{\partial R^2}-E\right)F_\mu(R)+\sum_\nu V_{\mu\nu}(R)F_\nu(R)=0. \quad (5)$$

Integration of Eq. (5) proceeds by decomposing the inner region $0\leqslant R\leqslant R_M$ into many sectors (typically a few hundred) within each of which the hyperradius R in $\phi_\mu(R;\alpha,\Omega)$ is taken to be constant. The solutions propagated out to R_M are then matched to the asymptotic solutions [Eq. (1)].

Extension of *ab initio* computational methods based on discretization of the continuum to higher energies faces the problem of the rapid growth of the number of open channels. One strategy to limit the number of open channels is to decrease the matching radius R_M with increasing energy. For smaller box size, however, the energy separation of the pseudostates becomes larger, i.e., the discrete density of pseudostates is reduced. This, in turn, limits the accuracy with which the double-ionization continuum can be represented. Figure 1 illustrates the discrete representation of the energy sharing between the two electrons at a photon energy $E_{\rm ph}=1$ keV. It is this constraint that limits the present extension of the HSCC method to $E_{\rm ph}\leqslant 1$ keV (note that the energy distribution is symmetric about the midpoint $\epsilon_i/E=0.5$). At higher energies, perturbation theory as discussed below is expected to be more suitable. We used three different matching radii $R_M=40$, 30, and 20 for photon energies from 80 to 200 eV, from 200 to 330 eV, and from 330 eV to 1 keV, respectively while we kept the number of coupling channels fixed to 175. For overlapping energy intervals we have checked that the results for different R_M have converged to within 5%. One important feature of the present method is the near gauge independence of our calculated ionization cross sections. We used both length and acceleration forms of the dipole transition matrix in the calculation and they agree to within 3% of each other.

Turning now to high energies, we employ perturbation theory with a 3C wave function to describe the correlated final state. The 3C wave function was initially introduced to study the electron-impact excitation of hydrogen [17] and then ionization processes by electron or positron impact [18]. The 3C wave function has been shown to satisfy the boundary condition in the asymptotic region where the separation of all the Coulomb interacting particles tends to infinity [18]. This property, while of importance from the viewpoint of the formal theory of scattering, is of little practical relevance to the photoionization process, since the dominant contributions to the photoionization originate from small to intermediate interparticle distances. We therefore focus on the properties of the wave function in the *entire* coordinate space in the perturbative regime of small Sommerfeld parameters $Z/k_1\gg 1$ where k_1 is the velocity of the fast electron.

For a two-electron atomic system, assume that the wave function for a double continuum state has the form

$$\psi_f^{(-)}(\mathbf{r}_1,\mathbf{r}_2)=\phi_{\mathbf{k}_1}^{(-)}(\mathbf{r}_1)\phi_{\mathbf{k}_2}^{(-)}(\mathbf{r}_2)B^{(-)}(\mathbf{k}_{12},\mathbf{r}_{12}), \quad (6)$$

where $\phi_{\mathbf{k}_1}^{(-)}(\mathbf{r}_1)$ and $\phi_{\mathbf{k}_2}^{(-)}(\mathbf{r}_2)$ are incoming Coulomb waves of the two electrons, and $B^{(-)}(\mathbf{k}_{12},\mathbf{r}_{12})$ is a function to be determined. In Eq. (6) ψ_f^- is understood to be (anti)symmetrized. With this ansatz, the three-body Schrödinger equation for infinite nuclear mass,

$$\left(-\frac{1}{2}\nabla_1^2-\frac{1}{2}\nabla_2^2-\frac{Z}{r_1}-\frac{Z}{r_2}+\frac{1}{r_{12}}\right)\psi_f^{(-)}(\mathbf{r}_1,\mathbf{r}_2) =E\psi_{\mathbf{f}}^{(-)}(\mathbf{r}_1,\mathbf{r}_2), \quad (7)$$

is reduced to

$$\left(-\frac{1}{2}\nabla_{\mathbf{r}_{12}}^2+\frac{1}{2r_{12}}+(-i\mathbf{k}_{12}+Z\mathbf{M}_1-Z\mathbf{M}_2)\cdot\boldsymbol{\nabla}m_{\mathbf{r}_{12}}\right) \times B^{(-)}(\mathbf{k}_{12},\mathbf{r}_{12})=0, \quad (8)$$

where $\mathbf{k}_{12}$ is the relative momentum (velocity) of the two electrons and $\mathbf{M}_i$ is defined as a ratio of two hypergeometric functions of different order,

$$\mathbf{M}_i=\frac{(\hat{r}_i+\hat{k}_i)}{2}\frac{{}_1F_1[1+i\,\eta_i,2,-i(k_ir_i+\mathbf{k}_i\cdot\mathbf{r}_i)]}{{}_1F_1[i\,\eta_i,1,-i(k_ir_i+\mathbf{k}_i\cdot\mathbf{r}_i)]}. \quad (9)$$

Here $\eta_i=-Z/k_i$ with $i=1,2$. The important observation is that $\mathbf{M}_i$ are bounded, $|\mathbf{M}_i|\lesssim 2$, for *all* r_i and *all* angles $\theta_i=\cos^{-1}(\hat{\mathbf{k}}_i\cdot\hat{\mathbf{r}}_i)$. Figure 2 displays the radial and angular dependence of M_i for typical values of k_i representing a fast electron $(i=1)$ and a slow electron $(i=2)$ in the double continuum at $E=2$ keV. At high energies, the typical relative momentum between the fast and the slow electrons satisfies

$$k_{12}\gg Z. \quad (10)$$

Therefore, Eq. (8) can be simplified to

$$\left(-\frac{1}{2}\nabla_{\mathbf{r}_{12}}^2+\frac{1}{2r_{12}}-i\mathbf{k}_{12}\cdot\boldsymbol{\nabla}_{\mathbf{r}_{12}}\right)B^{(-)}(\mathbf{k}_{12},\mathbf{r}_{12})=0. \quad (11)$$

The solution of this equation is nothing but the distortion factor to a plane wave due to the electron-electron interaction,

$$B^{(-)}(\mathbf{k}_{12},\mathbf{r}_{12})=D^{(-)}(\mathbf{k}_{12},\mathbf{r}_{12}), \quad (12)$$

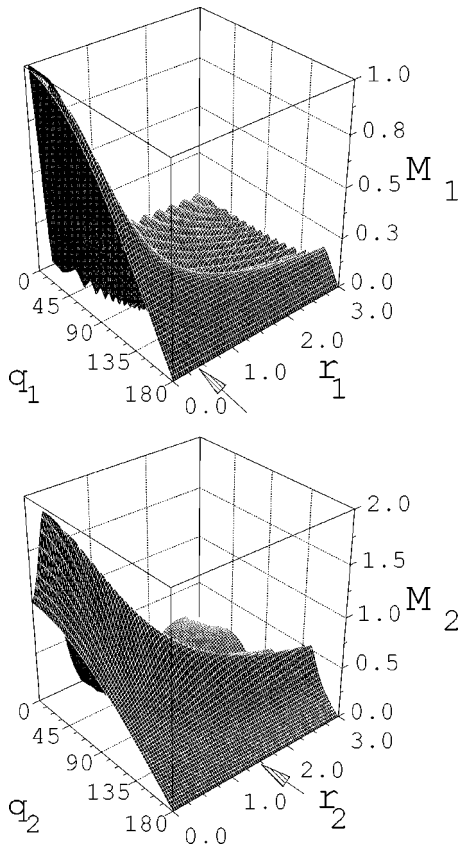

FIG. 2. Behavior of $M_i(r_i,\theta_i)$ as a function of radial r_i and angle θ_i coordinates at $E=2$ keV with an asymmetric energy distribution: fast electron $E_1=1950$ eV (upper panel) and slow electron $E_2=50$ eV (lower panel). Arrows indicate dominant regions for the dipole matrix element.

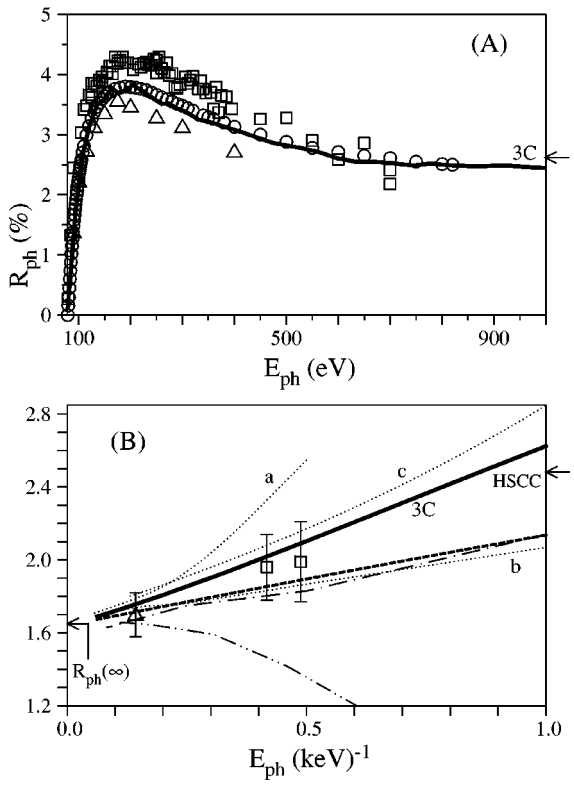

FIG. 3. Comparison of the ratio $R_{\rm ph}$ calculated by the present methods (solid curves) with experiments. (A) HSCC calculation below $E_{\rm ph}=1$ keV. Experimental data: circles from Ref. [4]; triangles from Ref. [3]; squares from Ref. [2]. The arrow indicates the ratio obtained from the 3C method at $E_{\rm ph}=1$ keV (lower panel). (B) The 3C calculation above $E_{\rm ph}=1$ keV. Experimental data: squares from Ref. [2]; triangles from Ref. [22] with Compton scattering excluded. Other calculations: chained curve by MBPT [13]; dash-double-dotted curve by the dipole response function [15]. Previous calculations employing the 3C function (dotted curves). Curve a, Ref. [6]; curve b, Ref. [14]; curve c, Ref. [8]. The dashed curve is the present calculation with only the monopole term included. The arrow indicates the ratio calculated by the HSCC method at 1 keV (upper panel).

where

$$D^{(-)}(\mathbf{k}_{12},\mathbf{r}_{12})=e^{-\pi\eta_{12}/2}\Gamma(1-i\eta_{12}) \times {}_1F_1[i\eta_{12},1,-i(k_{12}r_{12}+\mathbf{k}_{12}\cdot\mathbf{r}_{12})], \tag{13}$$

with $\eta_{12}=1/2k_{12}$. Consequently, $\psi_f^{(-)}(\mathbf{r}_1,\mathbf{r}_2)$ in Eq. (6) becomes the 3C wave function [18]. Taking into account that the energy distribution in the double photoionization is extremely asymmetric at high energies (Fig. 1), the condition, Eq. (10), is then reduced to $E_{\rm ph}\gg Z^2$. The 3C function is therefore the correct three-body final state in the full coordinate space, provided that the photon energy is high and the energy sharing is asymmetric. Moreover, the 3C wave function satisfies the cusp conditions in both the electron-nucleus and electron-electron coordinates near the origin. This is crucial for the photoionization shake-off process, since it is governed by the behavior of the wave functions at small interparticle distances.

The initial-state wave function is expanded in a correlated Hylleraas basis set [19]

$$\psi_i(\mathbf{r}_1,\mathbf{r}_2)=e^{-\sigma(r_1+r_2)/2}\sum_{n,l,m} C_{nlm}\sigma^{n+l+m} \times(r_1+r_2)^l(r_1-r_2)^m r_{12}^n, \tag{14}$$

and is obtained by a variation of σ and of C_{nlm}. The use of both integer and half-integer for l and the explicit inclusion of r_{12} terms guarantee high accuracy and fast convergence. We use a total of 34 terms for which the photoionization result is found to converge. The initial-state energy obtained is $-2.903\,72$ and the Kato cusp conditions [20] are satisfied to high precision. The double-ionization cross section is calculated both directly and indirectly through a closure relation [6]. The two methods are found to agree to within 1% at the high energies studied here. Following the suggestion of Dalgarno and Sadgehpour [5], we employ in evaluation of $\sigma^+(n)$ the acceleration gauge at high energies that places the dominant weight on the final-state wave function at small distances from the nucleus.

The present approach differs from previous calculations employing 3C final states [6,8,14]. Unlike the calculation of Hino [14], who used the monopole term only, we include all contributing multipoles in the expansion of the distortion factor $D^{(-)}(\mathbf{k}_{12},\mathbf{r}_{12})$. Furthermore, we eliminate additional approximations in the evaluation of $D^{(-)}$ by the closure relation used by Andersson and Burgdörfer [6]. Finally, we use

a more accurate initial-state wave function than that in the calculation of Teng and Shakeshaft [8]. The ground-state correlation is crucial for double photoionization at high energies and becomes dominant in the high-energy limit.

The ratio $R_{\rm ph}$, calculated in the acceleration form, from the double-ionization threshold to 16 keV is presented in Fig. 3. At low and intermediate energies [Fig. 3(A)] the HSCC result agrees, from the threshold ($E_{\rm ph}\approx 80$ eV) to 800 eV, excellently with the recommended data obtained from several experimental data sets by Samson [4], and, within the error bars, also with the data of Dörner *et al.* [3]. The deviation from the experimental data of Levin *et al.* [2] at low energies may be accounted for by an erroneous use of spectral filters in that experiment [21]. At high energies [Fig. 3(B)] we present $R_{\rm ph}$ as a function of the inverse photon energy $E_{\rm ph}^{-1}$. The result of Teng and Shakeshaft [8] shows a somewhat similar energy dependence but lies systematically higher than our 3C result. This difference comes most likely from the initial-state wave function. In the calculation of Teng and Shakeshaft [8] an eight-parameter ground-state wave function is used with relative errors in the Kato cusp conditions of about 5% for the confluence of the electron-nucleus coordinates and 35% for the confluence of the electron-electron coordinates, while in the present calculation they are 0.001% and 9%, respectively. Our calculation proceeds by expanding the distortion factor $D^{(-)}$ in terms of partial waves in the $\mathbf{r}_{12}$ coordinates. The convergence of $R_{\rm ph}$ as a function of partial waves included is examined. Taking only the monopole term into account leads to results similar but not identical to Hino's calculations [14] and also to MBPT [13]. When all contributing partial waves are summed up ($l\leqslant 4$) we find excellent agreement with experimental data. Included are the measurements of Levin *et al.* [2] around 2 keV and of Spielberger *et al.* [22] at higher energies. In the latter data set, contributions from Compton scattering and photoionization are resolved and a direct comparison with calculations is possible. Even more remarkable, the present result merges with the HSCC calculation [Fig. 3(A)] at 1 keV. The relative deviation of about 5% between the HSCC ($R_{\rm ph}=2.48\%$) and the 3C wave function ($R_{\rm ph}=2.62\%$) lies within the theoretical errors of the two methods at this energy.

In summary, we have presented two complementary accurate calculations for the ratio of double- to single-ionization cross sections, $R_{\rm ph}$, covering the entire energy range for photon energy from the near-double-ionization threshold $E_{\rm ph}\approx 80$ eV to the nonrelativistic asymptotic limit. They agree with most recent experimental data in the whole energy region and with each other at intermediate energies to within 5%. We estimate the latter to be the measure for accuracy of the present theory.

This work was supported by the NSF and by U.S. DOE, Office of BES, Division of Chemical Science, under Contract No. DE-AC05-96OR22646 with LMERC.

[1] J. A. R. Samson, Z. X. He, L. Yin, and G. N. Haddad, J. Phys. B **27**, 887 (1994).
[2] J. C. Levin, G. B. Armen, and I. A. Sellin, Phys. Rev. Lett. **76**, 1220 (1996).
[3] R. Dörner *et al.*, Phys. Rev. Lett. **76**, 2654 (1996).
[4] J. A. R. Samson (private communications).
[5] A. Dalgarno and H. Sadeghpour, Phys. Rev. A **46**, 3591 (1992).
[6] L. R. Andersson and J. Burgdörfer, Phys. Rev. Lett. **71**, 50 (1993).
[7] M. A. Kornberg and J. E. Miraglia, Phys. Rev. A **48**, R3714 (1993).
[8] Z. Teng and R. Shakeshaft, Phys. Rev. A **47**, R3487 (1993).
[9] J. Z. Tang and I. Shimamura, Phys. Rev. A **52**, R3413 (1995).
[10] K. W. Meyer and C. H. Greene, Phys. Rev. A **50**, R3573 (1994).
[11] M. Pont and R. Shakeshaft, J. Phys. B **28**, L571 (1995).
[12] C. Pan and H. P. Kelly, J. Phys. B **28**, 5001 (1995).
[13] T. Ishihara, K. Hino, and J. H. McGuire, Phys. Rev. A **44**, R6980 (1991); K. Hino, T. Ishihara, F. Shimizu, N. Toshima, and J. H. McGuire, *ibid.* **48**, 1271 (1993).
[14] K. Hino, Phys. Rev. A **47**, 4845 (1993).
[15] R. C. Forrey, Z. Yan, H. R. Sadeghpour, and A. Dalgarno, Phys. Rev. Lett. **78**, 3662 (1997).
[16] J. Z. Tang, S. Watanabe, and M. Matsuzawa, Phys. Rev. A **46**, 2437 (1992); J. Z. Tang and I. Shimamura, *ibid.* **50**, 1321 (1994).
[17] L. Vainshtein, L. Presnyakov, and I. Sobelman, Zh. Eksp. Teor. Fiz. **45**, 2015 (1963) [Sov. Phys. JETP **18**, 1383 (1964)].
[18] M. Brauner, J. S. Briggs, and H. Klar, J. Phys. B **22**, 2265 (1989).
[19] C. Schwartz, Phys. Rev. **128**, 1146 (1962), and references therein.
[20] T. Kato, Commun. Pure Appl. Math. **10**, 151 (1957).
[21] J. Levin (private communication). A new experimental data set at low energies agrees excellently with the present HSCC calculation.
[22] L. Spielberger *et al.*, Phys. Rev. Lett. **74**, 4615 (1995).